Acta Oceanol. Sin., 2018, Vol. 37, No. 7, P. 1–7
DOI: 10.1007/s13131-018-1239-8
http://www.hyxb.org.cn
E-mail: hyxbe@263.net

A harmonic analyzed parameterization of tide-induced mixing for ocean models

WEI Zexun[1, 2]*, SUN Junchuan[1, 2], TENG Fei[1, 2], XU Tengfei[1, 2], WANG Yonggang[1, 2], XU Xiaoqing[1, 2], FANG Guohong[1, 2]

[1] The First Institute of Oceanography, State Oceanic Administration, Qingdao 266061, China

[2] Functional Laboratory for Regional Oceanography and Numerical Modeling, Qingdao National Laboratory for Marine Science and Technology, Qingdao 266237, China

Received 9 May 2018; accepted 28 May 2018

Abstract

The tide-induced mixing plays an important role in the regulation of ocean circulation. Numerical simulation of continental shelf circulation is found to exhibit an unreasonable vertical thermohaline structure without consideration of tide effects. In this study, we establish a harmonic analyzed parameterization of tide-induced (HAT) mixing, by which means to derive time-depended function of mixing coefficient based on harmonic analysis of the vertical mixing coefficient. By employing HAT mixing parameterization scheme, a series of numerical experiments are conducted for the Yellow Sea. Numerical results show that an ocean circulation model with the HAT mixing involved is capable of reproducing the reasonable thermohaline structure of the Yellow Sea Cold Water Mass, similar to structures produced by explicit tidal forcing on the open boundary. The advantage of the HAT method is its faster computation time, compared with models that directly resolve explicit tidal motion. The HAT parameterization for the tide-induced mixing has potential to improve both the accuracy and efficiency of ocean circulation and climate models.

Key words: tide-induced mixing, harmonic analysis, parameterization, ocean circulation models, Yellow Sea Cold Water Mass

Citation: Wei Zexun, Sun Junchuan, Teng Fei, Xu Tengfei, Wang Yonggang, Xu Xiaoqing, Fang Guohong. 2018. A harmonic analyzed parameterization of tide-induced mixing for ocean models. Acta Oceanologica Sinica, 37(7): 1–7, doi: 10.1007/s13131-018-1239-8

1 Introduction

Tides play an important role in the regulation of ocean circulation, especially in continental shelf areas. Tide-induced mixing has a dominant influence on the near-bottom waters of the frontal zone (Rockwell, 1995). In the case of the Yellow Sea (YS), tides have strong currents and large tidal amplitudes, producing strong tide-induced mixing. This generates horizontal tidal mixing fronts, which produce a large horizontal density gradient. Xia et al. (2004) proposed that the subsurface cyclonic gyre associated with an isolated bottom cold water dome in the central YS is mainly a quasi-geostrophic flow along tide-induced temperature fronts based on a prognostic coupled wave-tide-circulation model. Moon et al. (2009) investigated the influence of tidal forces on seasonal variation of the YS circulation and proposed that the summer circulation results from a combination of the strong tidal residual current associated with stratified tidal rectification and the density gradient associated with the surface front and bottom cold water dome. According to a numerical study by Lü et al. (2010), strong tidal mixing plays an important role in the formation of vertical circulation in the YS in summer, with different tidal mixing effects between shallow and deep water leading to conspicuous fronts. Ren et al. (2014) studied different tidal effects on thermal fronts in the YS in summer, proposing that the front around the southwestern Korean Peninsula is mainly driven by tide-induced upwelling; the Shandong Peninsula front is mainly induced by tidal mixing, while the Subei Bank front is the result of both effects.

An appropriate way to incorporate the effects of tide-induced mixing in an ocean circulation model is to directly include tidal forcing on the open boundary (Xia et al., 2004; Moon et al., 2009; Lü et al., 2010; Ren et al., 2014). Given that the time-scale for tides is much smaller than for ocean circulation, the time step for the integration of an ocean circulation model with tidal forcing is one order of magnitude smaller than that of a stand-alone ocean circulation model. Consequently, the ocean circulation model requires additional computation time to include tidal forcing. An alternative is to import a parameterization scheme to describe the tide-induced mixing in ocean circulation models, instead of running an independent tide model. Mixing in ocean models can be described as eddy viscosity and eddy diffusion, respectively. In the case of vertical mixing, there are parameterization schemes based on bulk model, instability theory, Prandtl mixing length theory, turbulence closure model, etc.

Kraus and Turner (1967) proposed a bulk model for the upper mixed layer, by assuming that the vertical mixing is induced by entrainment/detrainment processes (Gaspar, 1988). Price et

Foundation item: The National Key Research and Development Program of China under contract No. 2017YFC1404201; the National Natural Science Foundation of China (NSFC) under contract Nos 41606040 and 41606036; the NSFC-Shandong Joint Fund for Marine Science Research Centers under contract No. U1606405; the National High Technology Research and Development Program (863 Program) of China under contract No. 2013AA09A506.
*Corresponding author, E-mail: weizx@fio.org.cn

al. (1986) proposed a quasi-salb model (PWP) to represent the vertical mixing, by assuming that entrainment occurs if the bulk Richardson number smaller than 0.65 and/or the gradient Richardson number smaller than 0.25.

There are some limitations of the bulk mixed layer models. For example, the Kraus-Turner bulk models cannot resolve the vertical structure of dynamical and thermodynamical variables. The PWP model does not account for the direct effects of wind stirring. Chen et al. (1994) proposed a hybrid mixing scheme by combining the Kraus-Turner bulk model with the gradient Richardson number mixing criterion from the PWP model.

The most common class of vertical mixing scheme employed in ocean models involves K theory, which assumes the vertical mixing as a function of eddy diffusivity and viscosity coefficients times the vertical gradient of mean quantities or as the functions of the gradient Richardson number (Pacanowski and Philander, 1981). Another approach is described as the turbulence closure scheme by Mellor and Yamada (1982), which introduces a hierarchy of prognostic equations used to solve for various turbulence fields. Large et al. (1994) introduced the K-profile parameterization (KPP) scheme to the ocean models, by considering both local and non-local mixing.

To date, most of the existing parameterization schemes for the tide-induced mixing employ a constant coefficient or a vertically varied coefficient to represent mixing, in addition to the eddy viscosity coefficient (Li et al., 2003). Li et al. (2006) proposed a parameterization scheme for different tidal currents having variable depth and amplitude. However, their scheme does not consider temporal variation of the tide-induced mixing coefficient caused by the periodic fluctuation of tides. Moon et al. (2009) studied the role of the tide-induced mixing in the YS circulation but only considered the tidal mixing effects as a function of the M_2 tide constituent.

Given the fact that tidal fluctuation is periodic, with typical diurnal and semidiurnal periods, tide-induced mixing should be time dependent, reflecting tidal fluctuation. In this study, a parameterization scheme is established, which provides a tide-induced mixing coefficient having both temporal and spatial variations based on the harmonic analysis. Our model configuration is presented in Section 2. A harmonic analysis of tide-induced (HAT) mixing is given in Section 3. Section 4 provides results of a series of numerical experiments for the Yellow Sea Cold Water Mass (YSCWM), based on the Regional Ocean Model System (ROMS). A discussion and summary are given in Section 5.

2 Model configuration

The ROMS model set up and modifications used in this study are outlined below. The model region covers the Bohai Sea, the YS, and part of the East China Sea (28°–41°N, 117.5°–127°E), with a horizontal resolution of (1/12)° by (1/12)° and 26 vertical levels. The topography of the model is interpolated from the global ETOPO1 dataset. Monthly climatological data (monthly mean sea surface temperature, wind stresses, net heat flux, surface solar shortwave radiation, net fresh water flux, and sea surface salinity) from the Comprehensive Ocean–Atmosphere Data Set (COADS) are used to force the model. Eight principal tide constituents (M_2, S_2, N_2, K_2, K_1, O_1, P_1 and Q_1) are added at the open boundary, and the tidal amplitude and lag are derived from the Global Inverse Tide Model dataset (Egbert and Erofeeva, 2002). Lateral open boundaries (temperature, salinity, sea level and velocity) and initial conditions were obtained by interpolation the simulation result of Yang et al. (2011, 2012). The Changjiang (Yangtze) River is included as a freshwater source, using the climatological monthly mean discharge measured at the Datong observation station.

The Mellor-Yamada 2.5 turbulence closure scheme with the Galperin et al. (1988) modifications as described in Allen et al. (1995) is applied in the model with the common setting. This closure scheme adds two prognostic equations, one for the turbulent kinetic energy, and one for the turbulent kinetic energy times a length scale. The vertical mixing coefficients (A_v) calculated by the Mollor-Yamada 2.5 level turbulence closure scheme are used for further analysis.

3 Parameterization of the vertical mixing coefficient

Tidal fluctuation is subject to diurnal and semidiurnal cycles. As a result, tide-induced mixing is expected to show temporal variation accordingly. In this case, the A_v times series are extracted using the modeling results for five representative stations: Sta. a (39°N, 120°E; 21 m; Bohai Sea), Sta. b (35°N, 122°E; 50 m; Yellow Sea), Sta. c (35°N, 124°E; 78 m; Yellow Sea), Sta. d (35°N, 125°E; 74 m; Yellow Sea), and Sta. e (33°N, 124°E; 50 m; East China Sea). Figure 1 provides the time series of the A_v values at these stations, showing significant periodic fluctuations, with the typical periods of around 6.15 and 8.28 h (Fig. 2).

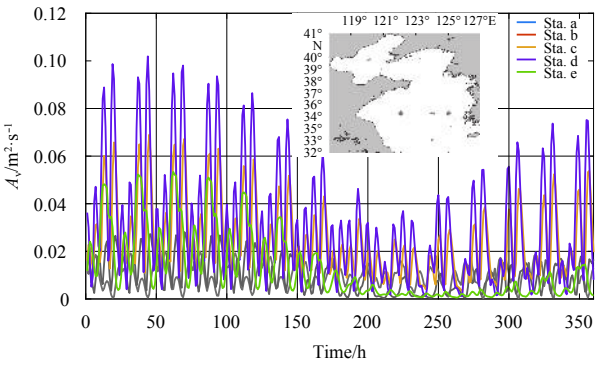

Fig. 1. Time series showing fluctuation of the vertical mixing coefficients (A_v) at five stations.

Figure 3 shows the vertical profiles of the A_v at these five stations, the A_v is parabolic within the mixed layer, but is 0 above and below the mixed layer. We selected the maximum value of the mixing coefficient for detailed analysis.

Analysis of the A_v shows it is periodic, reflecting tidal fluctuations, while its vertical structure is parabolic. Therefore, we can suppose that the A_v at each grid point (m, h) is a function of depth and the harmonic constant:

$$A_v(m,h) = M_h + \left(\sum_{i=1}^{P} + \sum_{i=P+1}^{P+Q}\right) A_i \cos(\omega_i t - G_i), \qquad (1)$$

where (m, h) stands for the location and depth; the subscript i stands for a given tidal constituent, ω_i is the angular speed of the given tidal constituent; A_i and G_i are the amplitudes and Greenwich phase-lags of the A_v, respectively; M_h is the mean value of the A_v at depth h; $\sum_{i=1}^{P}$ is the sum of P principal tidal constituents; $\sum_{i=P+1}^{P+Q}$ is the sum of Q subordinate tidal constituents. Equation (1) can be rewritten as

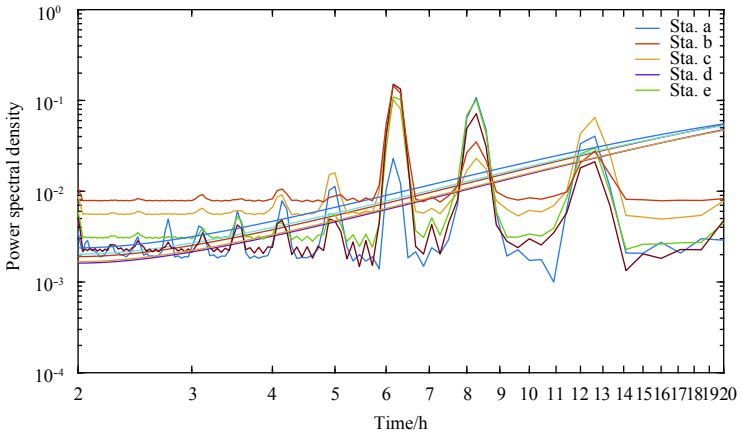

Fig. 2. Power spectra density of the vertical mixing coefficients (A_v) time series at five stations. The lines cross the spectrum indicate the 95% significance level.

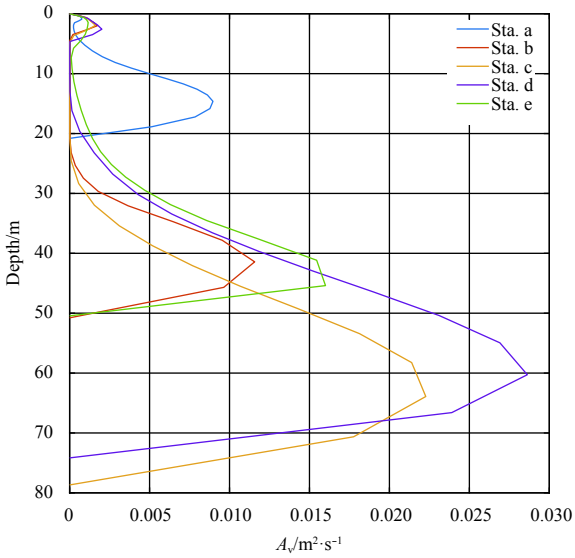

Fig. 3. Profiles of the vertical mixing coefficient (A_v) with depth at five stations.

$$A_v(m,h) = M_h + \left(\sum_{i=1}^{P} + \sum_{i=P+1}^{P+Q}\right)\left[\alpha_l(t)X_l + \beta_l(t)Y_l\right], \quad (2)$$

where

$$\left.\begin{aligned}\alpha_l(t) &= \cos(\omega_l t)\\ \beta_l(t) &= \sin(\omega_l t)\end{aligned}\right\}, \quad (3)$$

$$\left.\begin{aligned}X_l(t) &= A_l\cos G_l\\ Y_l(t) &= A_l\sin G_l\end{aligned}\right\}. \quad (4)$$

We carried out harmonic analysis of the time series of the A_v at each of the five stations. The harmonic analysis of A_v values for Sta. c (35°N, 124°E; Yellow Sea) yielded 29 harmonic constants. The maximum amplitudes for tidal constituents MSF, MS_3 and M_4 at Sta. c are given in Table 1. The results are similar at different water depths and stations.

According to Eq. (1), it is possible to reconstruct a time series of the A_v values (hereafter the reconstructed A_v is referred to as the HAT A_v) with an arbitrary length, which matches well with the original A_v time series extracted directly from the tide model (hereafter the original A_v is referred to as the model A_v) (Fig. 4). The HAT A_v is generally slightly smaller than the model A_v (Fig. 4). This is because the model A_v contains the effect of wind, and the HAT A_v does not contain all the tidal constituents, resulting in slight error. The correlation between model and HAT A_v values yielded a correlation coefficient of 0.89, a mean absolute error of 3×10^{-3} m²/s, a mean relative error of 3.5%, and a root-mean-square error of 5×10^{-3} m²/s.

Using the HAT A_v values, we obtained the A_v distribution for the study region, and the final equation can be written as follows:

$$A_v(\mathrm{lon},\mathrm{lat},h) = \sum_{i=1}^{P} A_i\cos(\omega_i t - G_i) + M_h, \quad (5)$$

where lon and lat are short for longitude and latitude, respectively.

4 Application of the harmonic parameterization

4.1 *Experimental design*

In this section, we assessed whether the HAT parameterization can be employed within an ocean circulation model to evaluate the effects of the tide-induced mixing.

To evaluate the effects of the harmonic parameterization, we introduced the following parameters into the ROMS model:

$$\left.\begin{aligned}A_v &= A_{v,\,\mathrm{model}} + A_{v,\,\mathrm{HAT}}\\ A_t &= A_{t,\,\mathrm{model}} + A_{t,\,\mathrm{HAT}}\end{aligned}\right\}, \quad (6)$$

where A_v and A_t are the vertical mixing coefficients for momentum and tracers, respectively. $A_{v,\,\mathrm{model}}$ and $A_{t,\,\mathrm{model}}$ represent the A_v and A_t produced by ROMS based on the Mellor–Yamada level 2.5 vertical mixing closures scheme, and $A_{v,\,\mathrm{HAT}}$ is the tide induced A_v calculated by HAT mothed. Generally, the A_t is about one-tenth of the A_v. Therefore, the $A_{t,\,\mathrm{HAT}}$ is simply defined as one-tenth of the $A_{v,\,\mathrm{HAT}}$ value.

The three cases shown in Table 2 were designed to investigate the suitability of the HAT method. In Case 1, the model runs with all forcings on (control run as described in Section 2); Case 2

Table 1. Harmonic constants of the vertical mixing coefficient (A_v) at Sta. c.

Constituent	Amplitudes/m^2·s^{-1}	Phase-lags/(°)	Constituent	Amplitudes/m^2·s^{-1}	Phase-lags/(°)
MSF	0.009 010	146.26	MK_3	0.008 063	294.64
$2Q_1$	0.002 119	297.21	SK3	0.001 857	47.67
Q_1	0.000 857	147.53	MN4	0.002 937	73.00
O_1	0.006 403	219.28	M_4	0.007 676	152.95
NO_1	0.001 024	350.80	MS4	0.004 058	284.97
K_1	0.006 076	128.56	S_4	0.000 593	43.17
J_1	0.000 160	336.22	2MK5	0.000 961	173.24
OO_1	0.001 055	169.00	2SK5	0.000 161	60.70
UPS1	0.000 375	356.02	2MN6	0.000 262	135.13
N_2	0.001 016	14.74	M_6	0.000 544	181.94
M_2	0.004 277	120.17	2MS6	0.000 789	334.85
S_2	0.001 863	272.50	2SM6	0.000 132	88.00
ETA2	0.000 140	93.27	3MK7	0.001 020	335.28
MO3	0.003 052	19.96	M_8	0.000 333	182.21
M_3	0.001 555	128.30			

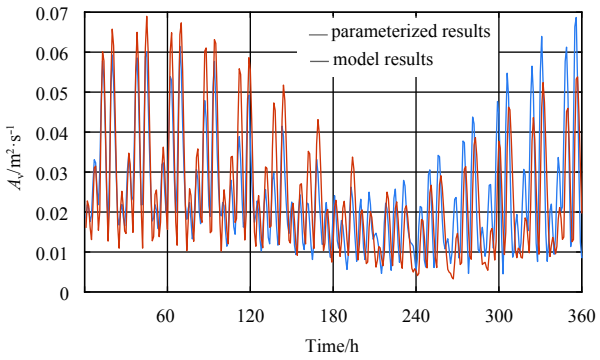

Fig. 4. Comparison of vertical mixing coefficients (A_v) from HAT parameterized (blue) and model (red) results.

is the same as Case 1 but without tidal forcing; while Case 3 is the same as Case 1 but uses the HAT mixing coefficient instead of tidal forcing. The differences between Case 2 and Case 3 show the effects of the HAT mixing. All cases were integrated over 10 years and the results of the last year were analyzed in our study.

4.2 *Experimental results*

The simulated temperature of the section along 35°N (a typical section of the YSCWM) in August is shown in Fig. 5. The main hydrographic features of the YS in summer is a stable low temperature water mass at the bottom of the YS, associated with a strong thermocline and temperature fronts (Xia et al., 2004). As shown in Fig. 5a, the temperature of the upper layer is relatively high, while the temperature of the bottom layer (especially in the Yellow Sea Trough) is low, forming strong stratification. Strong temperature fronts emerge on the eastern and western slopes, which produce a large horizontal density gradient. The temperature structure is vertically uniform, implying that the whole water column is fully mixed. This is because tides induce strong mixing and upwelling along the bottom slope (Fig. 6a). These mechanisms can raise the bottom cold water to the sea surface. In addition, the simulated A_v distribution along 35°N shows that the vertical mixing is strong in the near-bottom layer, with highest values on the eastern slope.

Comparing the results of Case 2 with the control run (Case 1) shows that without tidal forcing the temperature structure is approximately horizontal (Fig. 5b) and the temperature fronts disappear. This is because the vertical mixing and the upwelling are considerably weaker without tidal forcing (Fig. 6b).

Table 2. Experimental cases modeled in this study

Case	Forcing
1	control
2	no tide
3	no tide but with HAT Parameterization

In comparison, while HAT A_v are imported into the model, the simulated vertical structure of the temperature along 35°N (Fig. 5c) is similar to the control run. Figures 5d and 6d show the differences between the simulated temperature and the A_v for Case 3 and the control run, respectively. These differences mainly occur along the slopes on both sides of the study region, which may be attributed to the absence of tide-induced upwelling and bottom friction.

Figure 7 shows the simulated horizontal distributions of vertically averaged velocity magnitude (cm/s) in August of the three cases. The main hydrographic feature in the YS in summer is the cyclonic gyre associated with an isolated bottom cold water dome (Fig. 7a). This circulation becomes an anticyclonic gyre in the absence of tidal forcing (Fig. 7b). Moreover, when the HAT parameterization is introduced into the model, the circulation in the western YS is cyclonic, as in Case 1, but is relatively weak. The circulation in the eastern YS flows northward along the Korean Peninsula. Moon et al. (2009) argued that this is because the effect of parameterized tides neglects the contribution of tidal residual current, which is intensified in the subsurface layer when there is summer stratification. Figure 7d shows the difference in vertically averaged velocity in August between Cases 3 and 2. In general, the effect of the tide-induced mixing on driving the cyclonic gyre is the same order of magnitude as that of the tidal residual current.

Nevertheless, the simulated vertical distribution of the temperature based on the HAT parameterization shows a similar pattern to that of tidal forcing, suggesting the feasibility of introducing the HAT parameterization scheme into general ocean circulation models or climate models to optimize computation time.

5 Summary

In this study, we proposed a harmonic analyzed parameteriz-

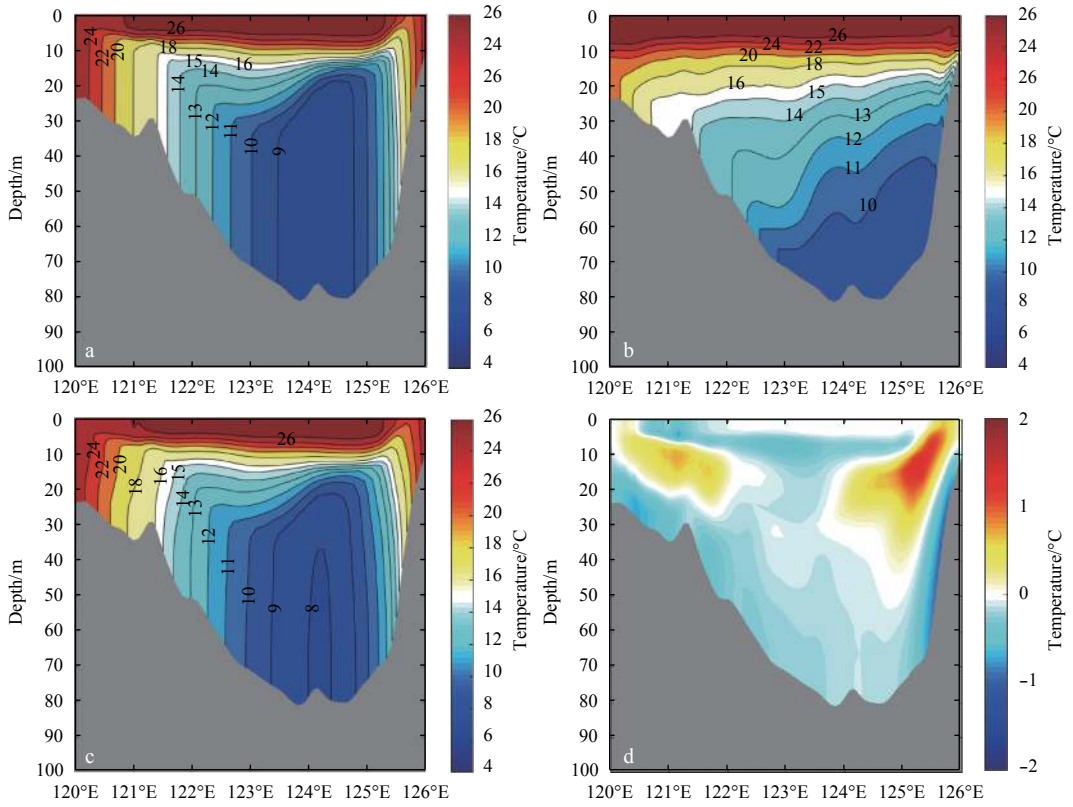

Fig. 5. Simulated temperature structures along 35°N in August for Case 1 (a), Case 2 (b), and Case 3 (c). Differences of temperature between Cases 3 and 1 along 35°N in August are shown in Fig. 5d.

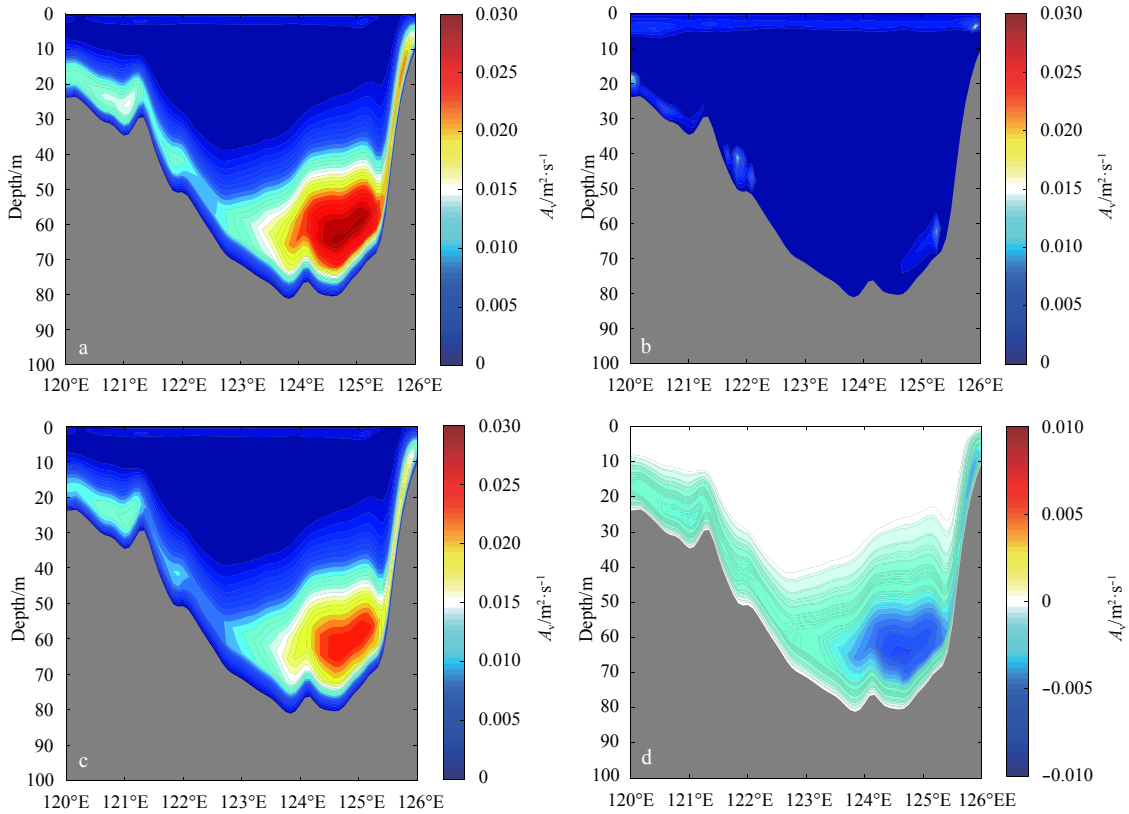

Fig. 6. Simulated vertical mixing coefficients (A_v) along 35°N in August for Case 1 (a), Case 2 (b), and Case 3 (c). Differences of A_v between Cases 3 and 1 along 35°N in August are shown in Fig. 6d.

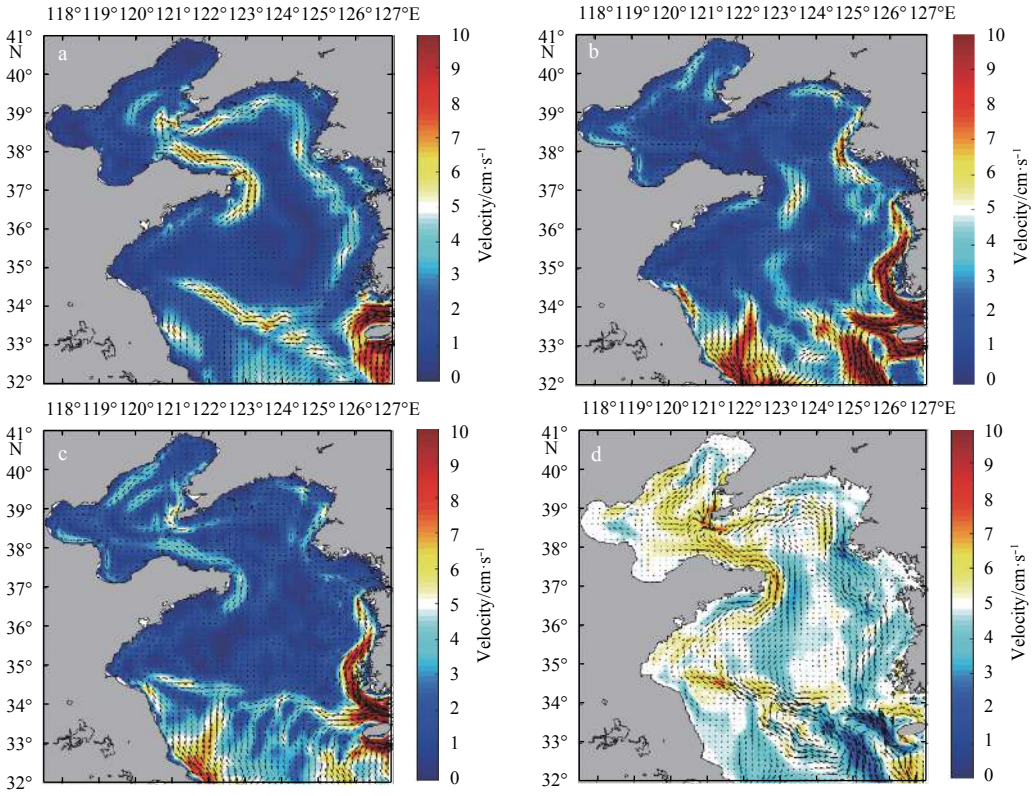

Fig. 7. Simulated horizontal distributions of vertically averaged velocities in August for Case 1 (a), Case 2 (b), and Case 3 (c). Differences of vertically averaged velocities in August between Cases 3 and 2 are shown in Fig. 7d. Shadings indicate the magnitude of velocity.

ation scheme for tide-induced mixing. Using the harmonic analysis, we derived the harmonic constants of the eddy viscosity coefficient. The harmonic constants were used to reconstruct a longer time series of eddy viscosity coefficient values. By employing the HAT parameterization in a regional ocean model for the YS, we showed that it is of capable of reproducing the vertical structure of the temperature, comparable to results obtained with tidal forcing on the open boundary. The advantage of the HAT parameterization is that it considers the effects of the tide-induced mixing in ocean models but does not require the tidal forcing. Therefore, it is expected to reduce computation time in ocean and climate models. In this study, we estimated that the time step for integration in our Case 3 experiment, which employed the HAT parameterization scheme, could be set to a maximum value of 1 500 s. In comparison, the maximum time step for our Case 1 experiment, including explicit tidal forcing, was only 400 seconds. Consequently, the wall time is 26.4 h and 10.5 h for one-month simulations in Cases 1 and 3, respectively, using 240 CPUs on the HPCC platform at the Shenzhen National Supercomputing Center.

We note that the simulated temperatures in Cases 1 and 3 were not identical along a section orientated 35°N, revealing differences of around 1.5°C at depths between 5–25 m near 125°E, and around 0.7°C near 121°E, respectively. These differences may be attributed to large differences of the vertical mixing coefficients between HAT and model A_v values, since that there are strong nonlinear processes along the coast, as well as the fact that our harmonic analysis does not consider tidal constituents at all frequencies.

The YS circulation in Case 3 showed a cyclonic circulation in the western YS associated with an isolated bottom cold water dome, reminiscent of our control case. However, it should be noted that circulation patterns offshore of the western side of the Korean Peninsula were not reproduced in Case 3. This is because the HAT parameterization does not include the effects of the tidal residual currents, which are important to the YS circulation in summer (Moon et al., 2009). In addition, there were marked differences in value between the HAT and model A_v in the Korean Peninsula offshore region.

References

Allen J S, Newberger P A, Federiuk J. 1995. Upwelling circulation on the Oregon continental shelf. Part I: Response to idealized forcing. Journal of Physical Oceanography, 25(8): 1843–1866

Chen Daka, Rothstein L M, Busalacchi A J. 1994. A hybrid vertical mixing scheme and its application to tropical ocean models. Journal of Physical Oceanography, 24(10): 2156–2179

Egbert G D, Erofeeva S Y. 2002. Efficient inverse modeling of barotropic ocean tides. Journal of Atmospheric and Oceanic Technology, 19: 183–204

Galperin B, Kantha L H, Hassid S, et al. 1988. A quasi-equilibrium turbulent energy model for geophysical flows. Journal of Atmospheric Sciences, 45(1): 55–62

Gaspar P. 1988. Modeling the seasonal cycle of the upper ocean. Journal of Physical Oceanography, 18(2): 161–180

Kraus E B, Turner J S. 1967. A one-dimensional model of the seasonal thermocline II. The general theory and its consequences. Tellus, 19(1): 98–106

Large W G, McWilliams J C, Doney S C. 1994. Oceanic vertical mixing: a review and a model with a nonlocal boundary layer parameterization. Reviews of Geophysics, 32(4): 363–403

Li Donghui, Zhang Ming, Wang Chunfu. 2003. Some technical problems in oceanic general circulation model. Journal of PLA Uni-

versity of Science & Technology (in Chinese), 4(4): 76–81

Li Mingkui, Hou Yijun, Qiao Fangli. 2006. Parameterization of the tide-induced vertical eddy viscosity coefficients. Progress in Natural Science (in Chinese), 16(1): 55–60

Lü Xingang, Qiao Fangli, Xia Changshui, et al. 2010. Upwelling and surface cold patches in the Yellow Sea in summer: effects of tidal mixing on the vertical circulation. Continental Shelf Research, 30(6): 620–632

Mellor G L, Yamada T. 1982. Development of a turbulence closure model for geophysical fluid problems. Reviews of Geophysics and Space Physics, 20(4): 851–875

Moon J H, Hirose N, Yoon J H. 2009. Comparison of wind and tidal contributions to seasonal circulation of the Yellow Sea. Journal of Geophysical Research: Oceans, 114(C8): C08016

Pacanowski R C, Philander S G H. 1981. Parameterization of vertical mixing in numerical models of tropical oceans. Journal of Physical Oceanography, 11(11): 1443–1451

Price J F, Weller R A, Pinkel R. 1986. Diurnal cycling: observations and models of the upper ocean response to diurnal heating, cooling, and wind mixing. Journal of Geophysical Research: Oceans, 91(C7): 8411–8427

Ren Shihe, Xie Jiping, Zhu Jiang. 2014. The roles of different mechanisms related to the tide-induced fronts in the Yellow Sea in summer. Advances in Atmospheric Sciences, 31(5): 1079–1089

Rockwell G W. 1995. Tide-induced mixing in the Amazon frontal zone. Journal of Geophysical Research: Oceans, 100(C2): 2341–2353

Xia Changshui, Qiao Fangli, Zhang Mengning, et al. 2004. Simulation of double cold cores of the 35°N section in the Yellow Sea with a wave-tide-circulation coupled model. Chinese Journal of Oceanology and Limnology, 22(3): 292–298

Yang Dezhou, Yin Baoshu, Liu Zhiliang, et al. 2011. Numerical study of the ocean circulation on the East China Sea shelf and a Kuroshio bottom branch northeast of Taiwan in summer. Journal of Geophysical Research: Oceans, 116(C5): C05015

Yang Dezhou, Yin Baoshu, Liu Zhiliang, et al. 2012. Numerical study on the pattern and origins of Kuroshio branches in the bottom water of southern East China Sea in summer. Journal of Geophysical Research: Oceans, 117(C2): C02014